

# 行政院國家科學委員會專題研究計畫 成果報告

中山醫學大學附設醫院的 Varian Clinac 21Ex 醫用直線加速器(6, 10, 15, 18 MeV)的中子通量及劑量估算  
研究成果報告(完整版)

計畫類別：個別型  
計畫編號：NSC 95-2623-7-040-001-NU  
執行期間：95年01月01日至95年12月31日  
執行單位：中山醫學大學醫學影像技術學系

計畫主持人：陳健懿

計畫參與人員：工讀生：邱怡菁、張維珍、黃琪雯

處理方式：本計畫可公開查詢

中華民國 96 年 03 月 29 日

# 行政院國家科學委員會專題研究計畫成果報告

中山醫學大學附設醫院的 Varian Clinac 21Ex 醫用直線加速器(6, 10, 15,18 MeV)的中子通量及劑量估算

Neutron Flux and Evaluations of Radiation Dose for Varian Clinac 21Ex of Medical Accelerator (6, 10, 15,18 MeV) of CSMUH

計畫編號：(NSC 95-2623-7-040-001-NU)

NSC 89-2212-E-014-022

執行期限：95 年 1 月 1 日至 95 年 12 月 31 日

主持人：陳健懿 執行機構及單位名稱：中山醫學大學 醫學影像暨放射科學系  
e-mail: ccy@csmu.edu.tw

## 1. 中文摘要

高能直線加速器(linac)產生電子及 x-光進行癌症治療，惟高出 10-MV 的加速器會經由光核反應產生巨量中子自靶區外釋，以銻片始活化法可利用產生的  $^{115}\text{In}(n,\gamma)^{116\text{m}}\text{In}$  度量中山醫學大學附設醫院放射腫瘤科 15、10 及 6-MV 的 Varian Clinac 21Ex 醫用直線加速器中治療室之熱中子通率( $\Phi_{\text{th}}$ )及估算熱中子劑量，結果發現 15-MV 在等中心點為  $(1.31\pm 0.09)\times 10^4$ ，是 6-MV  $(9.70\pm 0.88)\times 10^2$   $\text{cm}^{-2}\cdot\text{s}^{-1}$  的 13.5 倍。幾乎是等均勻分佈於整個治療室，但在機頭及天花板是等中心點的 20-50% 倍，歸因於中子受到鉛與天花板的散射及緩衝而增高，又因 6-MV 光子能量太低而無法測得  $\Phi_{\text{th}}$ 。最後以美國醫學物理學會 19 號報告來估計熱中子劑量，發現患者在 15-MV  $20\times 20$   $\text{cm}^2$  照野、2.5 分鐘 1000 cGy 治療下，熱中子劑量為每分鐘  $3.14\times 10^4$  pGy，換成每 x-光劑量為 39.3  $\mu\text{Sv}$ ，此換算值佔全部光子劑量的 0.0039%，與文獻值相符合。

關鍵字：醫用直線加速器，始活化法，熱中子通率

## Abstract

High-energy electron linear accelerators (linac) are routinely used to produce high energy electrons and x rays for cancer therapy. Accelerators operated at above 10-MV can produce dramatic neutrons through photonuclear reactions. Indium foil activation technique has been used employing for measurements at various locations in the treatment of Varian Clinac 21Ex of CSMUH of the 10 and 15-MV x-ray beam. The thermal neutron flux ( $\Phi_{\text{th}}$ ) using  $^{115}\text{In}(n,\gamma)^{116\text{m}}\text{In}$  reaction for the 15-MV,  $(1.31\pm 0.09)\times 10^4$  at isocenter is approximately 13.5 times than that of 10-MV beam,  $(9.70\pm 0.88)\times 10^2$   $\text{cm}^{-2}\cdot\text{s}^{-1}$  and nearly uniform throughout the treatment room.  $\Phi_{\text{th}}$  between the gantry head and the ceiling was 20-50 % higher than that at the isocenter because the neutrons were scattered and moderated with the lead shield in the gantry head. But  $\Phi_{\text{th}}$  can't be measured at 6-MV due to low x-ray energy of linac. According to AAPM 19, a patient receiving a photo dose of the order of 1000 cGy in 2.5 min treatment, the thermal

neutron absorbed doses are  $3.14 \times 10^4$  pGy  $\text{min}^{-1}$ . For 15-MV  $20 \times 20$   $\text{cm}^2$  field, the thermal neutron dose equivalent is 39.3  $\mu\text{Sv}$  per Gy X-ray dose and represents 0.0039% total dose which is consistent with the published.

Keyword: linear accelerator, foil activation technique, thermal neutron flux

## 1. Introduction

High-energy electron accelerators including the electron linear accelerator and the betatron are routinely used to produce high energy electrons and x rays for cancer therapy. Accelerators operated at above 10 MeV can produce neutrons through photonuclear reactions in the target, field-flattening filters, beam-defining collimators and other accelerator components, resulting in a mixed radiation field in the beam and the treatment room. The calculation of photoneutron yields and the subsequently induced photons in different components of medical accelerators and barriers has been extensively investigated to design shielding to protect personnel outside treatment rooms (Kase et al., 1998; Mao et al., 1996; Mao et al., 1997; McGinley et al., 1992). The contribution of neutrons and photons can be estimated for therapeutic and radiation safety purposes. Neutron fluences and the corresponding dose can also be measured experimentally and compared to the calculated results (Lin et al., 2001; Paredes et al., 1999; Palta et al., 1985; Gur et al., 1978; McGinley et al., 1976; Uwamino et al., 1986). Although the dose of photoneutrons is less than 0.5% of that of photons on the beam central axis at the depth of dose maximum, and less than 1% in treatment rooms (Paredes et al., 1999), the

rooms (Paredes et al., 1999), the photoneutrons can also produce activation of materials in treatment rooms to generate radioactive substances, which raise a concern about radiation safety.

## 2. Materials and Methods

### 2.1 Neutron activation of indium foils

The activation technique has been widely used for measurement of neutron fluxes and the corresponding doses (Knoll, 1989). Fast and thermal neutrons can be discriminated by irradiating appropriate foil materials and measuring the induced radioactivities (Lin et al., 2001; Paredes et al., 1999; Palta, et al., 1985; Deye and Young, 1977; Price and Holeman, 1978; Gur et al., 1987; McGinley et al., 1976; Uwamino et al., 1986). In the measurement of thermal neutrons, indium foils are commonly used due primarily to indium's high cross section and suitable half life ( $t_{1/2}=54.1\text{m}$ ) (Reus and Westmeier, 1983). In this study, indium foils were used to contour the distribution of thermal neutrons around a medical accelerator. The thermal neutron flux is defined and determined by measuring the induced radioactivities of indium foils, as follows:

$$A = \phi_{th} \times \sigma_{in} \times N_A \times \frac{m \times a}{M} \times (1 - e^{-\lambda t_i}) \times e^{-\lambda t_c},$$

where  $\phi_{th}$  is the thermal neutron flux ( $\text{cm}^{-2} \cdot \text{s}^{-1}$ );  $\sigma_{in}$  is the cross section of the activation reaction (161 barns);  $N_A$  is the Avogadro's number ( $6.02 \times 10^{23}$  in atoms per g-atom);  $m$  is the mass of indium foil (g);  $a$  the isotopic abundance of  $^{115}\text{In}$  (95.7%);  $M$  is the atomic weight of indium (114.82);  $\lambda$  is the disintegration rate of  $^{116\text{m}}\text{In}$  ( $2.135 \times 10^{-4} \text{ s}^{-1}$ );  $t_i$  is the irradiation

time, and  $t_c$  is the time duration between irradiation and measurement.

## 2.2 Neutron irradiation

Twenty indium foils (purity > 99.9%; 25 mm L×25 mm W×1 mm H) with an averaged mass of  $(4.86 \pm 0.07)$  g were used in the experiment. The foils were placed and distributed evenly in the vicinity of a medical accelerator (Clinac 21EX, Varian, Palo Alto, CA) for neutron irradiation. The electron accelerator provides dual photoenergies with accelerating voltages of 6 and 15 MV. The beam intensity was controlled by changing the pulse interval. Figure 1 displays a floor plan of the radiotherapy facility. The accelerator was operated at 15 MV for 2.5 min, delivering a dose of 1000 cGy at depth of dose maximum in a water-equivalent phantom with source-surface distance of 100 cm and the collimator open to a field size of  $20 \times 20$  cm<sup>2</sup>. For batch irradiation, all measured values were normalized to a reference foil, which was placed at the isocenter (0,0,0), which is exactly 100 cm below the x-ray target, such that the relative intensity of the thermal neutron in the treatment room can be simply described. The thermal neutron flux can be averaged by integrating thermal neutron flux with distance from the reference point.

## 2.3 Radioactivity measurement

The irradiated foils were immediately transferred to a gamma-ray spectrometric system, which consisted of a 30% high-purity germanium detector (GC3520, Canberra Industries, Meriden, CT, USA). The measured gamma-ray spectra were collected with a multichannel

analyzer (35-Plus, Canberra Industries, Meriden, CT, USA) and were further analyzed by gamma-ray spectrum software. The foils were placed immediately on the face of the detector for counting; the efficiency was determined to be 4.0% at the characteristic gamma-ray energy of 417 keV emitted from the activated nuclide  $^{116m1}\text{In}$ .

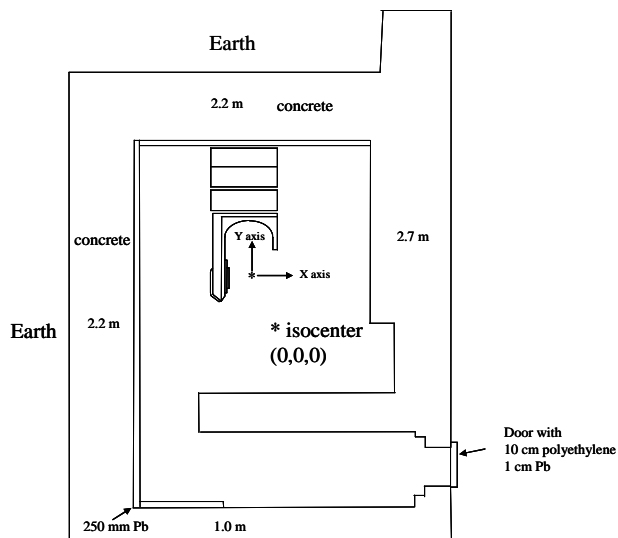


Figure 1, Schematic diagram of accelerator (Clinac 21EX) and room layout.

## 3. Results and Discussion

### 3.1 Thermal neutron flux distribution

The thermal neutron flux ( $\phi_{th}$ ) around the medical accelerator in the treatment room was determined by measuring the radioactivities of the indium foils and then calculated by Eq. (1). The thermal neutron flux at the linac isocenter, in the beam field, was determined to be  $1.31 \times 10^4$  cm<sup>-2</sup>·s<sup>-1</sup>, which is approximately the averaged value in the beam field over an area of  $20 \times 20$  cm<sup>2</sup>. Figure 2 presents the profile of the thermal neutron flux along the X axis, var-

ied from  $8 \times 10^3$  to  $1.4 \times 10^4$   $\text{cm}^{-2} \cdot \text{s}^{-1}$  with higher values in the beam field than outside it. Figure 3 presents the profile of the thermal neutron flux along the Y axis (0,y,0): the thermal neutron flux slightly declined with distance from the isocenter. It was remarkably shielded to under  $2 \times 10^3$   $\text{cm}^{-2} \cdot \text{s}^{-1}$  in the maze and  $5.9 \times 10^3$   $\text{cm}^{-2} \cdot \text{s}^{-1}$  near the wall behind the accelerator. The thermal neutron flux between the gantry head and the ceiling was 20-50 % higher than that at the isocenter because the neutrons were scattered and moderated with the lead shield in the gantry head, as illustrated in Fig. 4. The maximal value of  $2.0 \times 10^4$   $\text{cm}^{-2} \cdot \text{s}^{-1}$  in the treatment room was measured 1.5 m above the gantry head. The thermal neutron flux was slightly raised near the ground because the neutrons were moderated by scattering in the concrete material. The thermal neutron flux, ranging from  $8 \times 10^3$  to  $2 \times 10^4$   $\text{cm}^{-2} \cdot \text{s}^{-1}$ , seemed to be roughly uniform in the treatment room except in the maze (less than  $2 \times 10^3$ ). Integrating the thermal neutron flux distribution relative to the reference position yields an estimate of averaged neutron flux  $\bar{\Phi}_{\text{th}}$  in the room,  $1.02 \times 10^4$   $\text{cm}^{-2} \cdot \text{s}^{-1}$ .

Figure 5 compares the gamma-ray spectra for the irradiated indium foils placed inside and outside the beam field. The photopeak at 336 keV in Fig. 5(a) was from  $^{115\text{m}}\text{In}$ , and was associated mainly with high-energy photon interaction through an  $^{115}\text{In}(\gamma, \gamma')^{115\text{m}}\text{In}$  reaction (Chao et al., 2001).

### 3.2 Thermal neutron dose

According to American Association of Physicists in Medicine Task Group (AAPM)

report 19, the thermal neutron dose conversion factors are  $2.4 \text{ pGy min}^{-1} \text{ per n cm}^{-2} \text{ s}^{-1}$ . (Lin, 2001; AAPM No 19, 1986) Therefore, based on the data, a patient receiving a photo dose of the order of 1000 cGy in 2.5 min treatment, the thermal neutron absorbed dose are  $3.14 \times 10^4$   $\text{pGy min}^{-1}$ . It is assumed that the radiation weighting factor is set at 5 for thermal neutrons. (NCRP, No 16. 1993) For 15MV  $20 \times 20 \text{ cm}^2$  field, the thermal neutron dose equivalent at isocenter is 39.3 per Gy X-ray dose and represents 0.0039% total dose which is consistent with the results reported elsewhere. (Lin et al., 2001; Paredes et al., 1998; McCall et al., 1979)

### 3.3 Detection limit (DL) of foil activation technique

The detection limit (DL) of  $\Phi_{\text{th}}$  for  $^{116\text{m}}\text{In}$  in this study can be assessed as  $4.65 \times \text{DS} \times (\text{B}/t)^{1/2}$  where B is the background count rate at the 417 keV of  $^{116\text{m}}\text{In}$  and t is the counting period. (Chen, 2003; Currie, 1968) Hence, the detection sensitivity (DS) for  $^{116\text{m}}\text{In}$  can be calculated by dividing the counts of 417 keV by the  $\epsilon$  and the absolute  $\gamma$ -ray intensity. In the six-minutes counting period of 10 MV linac, the detection limit of  $\Phi_{\text{th}}$  is estimated to be  $50 \text{ n cm}^{-2} \text{ s}^{-1}$  under the experimental condition in this study. (Currie, 1968) It is highly feasible to use this technique for determination of  $\Phi_{\text{th}}$  among the treatment room of linac.

### Conclusion

The neutron activation method based on foil activation technique is an effective way to measure  $\Phi_{\text{th}}$  from electron medical accelerators. The results of  $\Phi_{\text{th}}$  measurements on Varian clinac 21EX accelerators are shown in Fig 4,

reporting  $\Phi_{th}$  as a function of distance from central axis.  $\Phi_{th}$  between the gantry head and the ceiling was 20-50 % higher than that at the isocenter because the neutrons were scattered and moderated with the lead shield in the gantry head. But  $\Phi_{th}$  can't be measured at 6-MV due to low x-ray energy of linac.

### Acknowledgements

The authors would like to thank the National Science Council of the Republic of China, Taiwan (Contract No. NSC-95-2623-7-040-001-NU). Radiotherapists C. C. Lu and S. T. Hsu of CSMUH are appreciated for their assistance in the operation of the accelerator.

### References

1. Chao, J. H., Hsu, P. C., Liu, H. M., 2001. Measurement of high dose rates by photon activation of indium foils. *Appl. Radiat. Isot.* 55, 549-556.
2. Chung, C., Chen, C. Y., Lin, C. S., Yeh, W. W., Lee, C. J., 1998. Rapid monitoring of gaseous fission products released from nuclear power stations. *J. Radioanal. Nucl. Chem.* 233, 281-284.
3. Currie, L. A., 1968. Limits for qualitative detection and qualitative determination. *Anal. Chem.* 40, 586.
4. Deye, J. A., Young, F. C., 1977. Neutron production from a 10MV medical linac. *Phys. Med. Biol.* 22, 90-94.
5. Gur, D., Rosen, J. C., Bukovitz, A. G., Gill, A. W., 1978. Fast and slow neutrons in an 18-MV photon beam from a Philips SL/75-20 linear accelerator. *Med. Phys.* 5(3), 221-222.
6. International Commission on Radiological Protection (ICRP), 1991. Annual limits on intake of radionuclides based on 1990 recommendations (ICRP 61 Report). Pergamon Press, Oxford.
7. Kase, K. R., Mao, X. S., Nelson, W. R., Liu, J. C., Kleck, J. H., Elsalim, M., 1998. Neutron fluence and energy spectra around the Varian Clinac 2100C/2300C medical accelerator. *Health Phys.* 74(1), 38-47.
8. Knoll, G. F., 1989. *Radiation Detection and Measurement* (2nd). John Wiley & Sons, New York.
9. Lederer, C. M., Shirley, V. S., 1977. *Table of Isotopes*, 7th edn. John Wiley & Sons, New York.
10. Lin, J. P., Chu, T. C., Lin, S. Y., Liu, M. T., 2001. The measurement of photoneutrons in the vicinity of a Siemens Primus linear accelerator. *Appl. Radiat. Isot.* 55, 315-321.
11. Mao, X., Kase, K. R., Nelson, W. R., 1996. Giant dipole resonance neutron yields produced by electrons as a function of target material and thickness. *Health Phys.* 70(2), 207-214.
12. Mao, X. S., Kase, K. R., Liu, J. C., Nelson, W. R., Klerk, J. H., Johnsen, S., 1997. Neutron sources in the Varian Clinac 2100C/2300C medical accelerator calculated by the EGS4 code. *Health Phys.* 72(4), 524-529.
13. McGinley, P. H., 1992. Photoneutron fields in medical accelerator rooms with primary barriers constructed of concrete and metals. *Health Phys.* 63(6), 698-701.
14. McGinley, P. H., Wood, M., Mills, M., Rodriguez, R., 1976. Dose levels due to neutrons in the vicinity of high-energy medical accelerators. *Med. Phys.* 3(6), 397-402.
15. Palta, J. R., Hogstrom, K. R., Tannanonta, C., 1985. Neutron leakage measurements from a medical linear accelerator. *Med. Phys.* 11(4), 498-501.
16. Paredes, L., Genis, R., Balcazar, M., Tavera, L., Camacho, E., 1999. Fast neutron leakage in 18 MeV medical electron accelerator. *Radiat. Meas.* 31, 475-478.